New hyperspectral discrimination measure for spectral characterization

Yingzi Du, MEMBER SPIE
Laboratory for Biometric Signal Processing
United States Naval Academy
Electrical Engineering Department
Annapolis, Maryland 21402
E-mail: ydu@usna.edu

Chein-I Chang, FELLOW SPIE
University of Maryland, Baltimore County
Department of Computer Science
and Electrical Engineering
Remote Sensing Signal and Image
Processing Laboratory
Baltimore, Maryland 21250

Hsuan Ren, MEMBER SPIE
National Central University
Department of Information Engineering
Center for Space and Remote
Sense Research
Chungli, Taiwan

Chein-Chi Chang
University of Maryland, Baltimore County
Department of Civil and Environmental
Engineering
Baltimore, Maryland 21250

James O. Jensen
Francis M. D'Amico
U.S. Army Edgewood Chemical and
Biological Center
Aberdeen Proving Ground, Maryland 21010

Abstract. The spectral angle mapper (SAM) has been widely used in multispectral and hyperspectral image analysis to measure spectral similarity between substance signatures for material identification. It has been shown that the SAM is essentially the Euclidean distance when the spectral angle is small. Most recently, a stochastic measure, called the spectral information divergence (SID), has been suggested to model the spectrum of a hyperspectral image pixel as a probability distribution, so that spectral variations among spectral bands can be captured more effectively in a stochastic manner. This paper develops a new hyperspectral spectral discrimination measure, which combines the SID and the SAM into a mixed measure. More specifically, let $\mathbf{r}$ and $\mathbf{r}'$ denote two hyperspectral image pixel vectors with their corresponding spectra specified by $\mathbf{s}$ and $\mathbf{s}'$. Then SAM($\mathbf{s}$,$\mathbf{s}'$) measures the spectral angle between $\mathbf{s}$ and $\mathbf{s}'$. Similarly, SID($\mathbf{s}$,$\mathbf{s}'$) measures the information divergence between the probability distributions generated by $\mathbf{s}$ and $\mathbf{s}'$. The proposed new measure, referred to as the SID-SAM mixed measure, can be implemented in two versions, given by SID($\mathbf{s}$,$\mathbf{s}'$)$\times$tan(SAM($\mathbf{s}$,$\mathbf{s}'$)) and SID($\mathbf{s}$,$\mathbf{s}'$)$\times$sin(SAM($\mathbf{s}$,$\mathbf{s}'$)), where tan and sin are the usual trigonometric functions. The spectral discriminability of such a mixed measure is greatly enhanced by multiplying the spectral abilities of the two measures. In order to demonstrate its utility, a comparative study is conducted among the SID-SAM mixed measure, the SID, and the SAM. Our experimental results have shown that the discriminatory ability of the (SID,SAM) mixed measure can be a significant improvement over the SID and SAM.
[DOI: 10.1117/1.1766301]

Subject terms: relative spectral discriminatory entropy (RSDE); relative spectral discriminatory power (RSDPW); relative spectral discriminatory probability (RSDPB); self-information; spectral angle mapper (SAM); spectral information divergence (SID); spectral information measure (SIM).

Paper TPR-030 received Nov. 13, 2003; accepted for publication Feb. 17, 2004.

1 Introduction

A remotely sensed image is usually collected by a number of spectral channels, each of which produces its individual and separate, but coregistered image. As a result, it is actually an image cube with each image pixel represented by a column vector of which each component is a pixel of an image acquired by a particular spectral channel. With recent remote sensing instruments such as imaging spectrometers, hundreds of spectral channels can be used to detect many material substances that generally cannot be resolved by multispectral imaging sensors. Such images are generally referred to as hyperspectral images, as opposed to multispectral images, which are acquired by tens of spectral channels. With so many additional spectral channels used for data acquisition, a hyperspectral image pixel vector provides more spectral information than does a multispectral image pixel vector. In many situations, such spectral information is valuable or even crucial in data analysis.

In order to capture and characterize the spectral properties provided in a single pixel vector by hundreds of spectral channels, a new stochastic measure, called the spectral information measure (SIM), was introduced in Refs. 1–4. It models the spectrum of a pixel vector as a probability distribution so that the spectral properties of the pixel vector can be further characterized by its statistical moments of any order, such as the mean, variance, skewness, and kurtosis. More importantly, by virtue of the SIM, many concepts in information theory are readily applied to spectral characterization. For example, the self-information derived from the SIM can be used to describe the information provided by a particular spectral channel within a pixel vector. Using such self-information, a discrimination measure, called the spectral information divergence (SID), can be derived and used to measure the spectral similarity between two pixel vectors.

In the remote sensing community, the spectral angle mapper (SAM) has been widely used as a spectral similarity measure for material identification. It calculates the angle between two spectra and uses it as a measure of discrimination. Another popular spectral similarity measure, Euclidean distance (ED), has also been used to calculate the distance between two spectra as a spectral similarity measure. It is shown in Refs. 1 and 2 that when the angle is

small, the SAM and ED yield very close results and they are essentially equivalent in terms of spectral discrimination. In contrast with the SID, the SAM and the ED are deterministic measures and consider a spectrum of a pixel vector as a vector rather than a probability distribution as modeled by the SIM.

This paper develops a new measure that combines the SID and SAM to form a mixed measure, called the SID-SAM mixed measure, which takes advantages of strengths of both measures. It can be implemented in two versions, $\mathrm{SID}(\mathbf{s},\mathbf{s}')\times\tan(\mathrm{SAM}(\mathbf{s},\mathbf{s}'))$ and $\mathrm{SID}(\mathbf{s},\mathbf{s}')\times\sin(\mathrm{SAM}(\mathbf{s},\mathbf{s}'))$, where $\mathbf{s}$ and $\mathbf{s}'$ are the spectra of the two pixel vectors $\mathbf{r}$ and $\mathbf{r}'$, and tan and sin are the tangent and sine trigonometric functions respectively. The SID-SAM mixed measure takes advantage of the strengths of both the SID and the SAM in spectral discriminability, in the sense that the spectral similarity and dissimilarity resulting from the mixed measure is considerably enhanced by multiplying the spectral abilities of the two measures. The reason for taking tangent or sine rather than cosine is to calculate the perpendicular distance between two vectors instead of the projection of one vector along the other vector. As a result, experimental results demonstrate that the simple SID-SAM mixed measure can be a significant improvement in discriminatory ability over the SID and the SAM.

The remainder of this paper is organized as follows. Section 2 briefly reviews the concept of spectral information measure developed in Refs. 1 and 2. Section 3 introduces three spectral discrimination measures: the SID, the SAM, and the proposed SID-SAM mixed measure. Section 4 describes some measures that can be used to evaluate the effectiveness of a spectral discrimination measure. Section 5 presents experimental results. Section 6 concludes with some remarks.

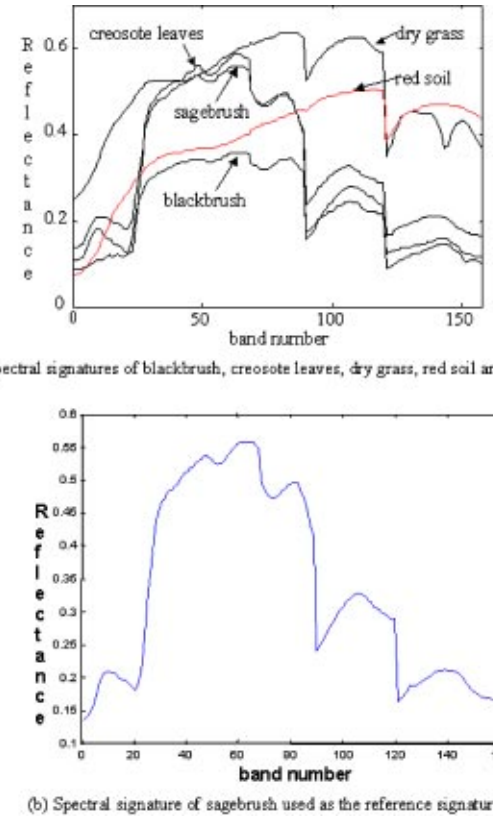

(a) Spectral signatures of blackbrush, creosote leaves, dry grass, red soil and sagebrush

(b) Spectral signature of sagebrush used as the reference signature

Fig. 1 Spectra of five AVIRIS reflectances: (a) Spectral signatures of blackbrush, creosote leaves, dry grass, red soil, and sagebrush. (b) Spectral signature of sagebrush, used as the reference signature.

2 Spectral Information Measure

The spectral information measure (SIM) is a newly developed stochastic measure,[1] which considers the spectral band-to-band variability as a result of uncertainty incurred by randomness. It models the spectral values of each hyperspectral image pixel vector as a random variable with the probability distribution obtained by normalizing its spectral histogram to unity. With this interpretation, the SIM is a measure of the spectral variability of a single hyperspectral image pixel vector based on interband correlation. It not only can capture the randomness of interband spectral changes of a pixel vector, but also can generate high-order statistics of spectral variations. Therefore, the SIM can be considered as a single-pixel-based information-theoretic measure.

For a given hyperspectral pixel vector $\mathbf{r}=(r_1,r_2,\ldots,r_L)^T$, each component r_j represents a pixel in the band image B_j, which is acquired by a certain wavelength ω_j in a specific spectral range. Let $\mathbf{s}=(s_1,s_2,\ldots,s_L)^T$ be the corresponding spectral signature (i.e., spectrum) of $\mathbf{r}$, where s_j represents the spectral signature of r_j in the form of either radiance or reflectance values. Suppose that $\{\omega_j\}_{j=1}^{L}$ is a set of L wavelengths, each of which corresponds to a spectral band channel. Then $\mathbf{r}$ can be modeled as a random variable by defining an appro-

Table 1 Discrimination values produced by SAM and SID.

		SAM				
		Blackbrush	Creosote leaves	Dry grass	Red soil	Sagebrush
SID	Blackbrush	0	0.1767	0.2575	0.4058	0.0681
	Creosote leaves	0.0497	0	0.4213	0.5714	0.1289
	Dry grass	0.0766	0.2298	0	0.2179	0.2968
	Red soil	0.1861	0.4154	0.0640	0	0.4515
	Sagebrush	0.0063	0.0303	0.0973	0.2340	0

Table 2 Discrimination values produced by SID(SIN) and SID(TAN).

		SID(SIN)				
		Blackbrush	Creosote leaves	Dry grass	Red soil	Sagebrush
SID(TAN)	Blackbrush	0	0.0087	0.0195	0.0735	0.0004
	Creosote leaves	0.0089	0	0.094	0.2247	0.0039
	Dry grass	0.0202	0.103	0	0.0138	0.0285
	Red soil	0.0800	0.2671	0.0142	0	0.1021
	Sagebrush	0.0004	0.004	0.0298	0.1135	0

priate probability space (Ω,Σ,P) associated with it, where Ω is a sample space, Σ is an event space, and P is a probability measure. In our case, $\Omega=\{\omega_1,\omega_2,\ldots,\omega_L\}$ is the sample space, Σ is the power set of Ω (i.e., the set of all subsets of Ω), and $\mathbf{r}(\omega_1)=s_j$.

In order to define a legitimate probability measure P for $\mathbf{r}$, we first assume that all components s_j associated with $\mathbf{r}$ are nonnegative. This is generally a valid assumption due to the nature of radiance or reflectance. With this assumption, we can normalize s_j to the range of [0, 1] as follows,

$$p_j=\frac{s_j}{\sum_{l=1}^{L}s_l}. \tag{1}$$

Using Eq. (1), we can further define a probability measure P for $\mathbf{r}$ by

$$P(\{\omega_j\})=p_j. \tag{2}$$

The probability vector $\mathbf{p}=(p_1,p_2,\ldots,p_L)^T$ is the probability mass function of the probability measure P and is the desired probability distribution of the pixel vector $\mathbf{r}$. By means of this probability interpretation, any pixel vector $\mathbf{r}=(r_1,r_2,\ldots,r_L)^T$ can be viewed as a single information source with its statistics governed by $\mathbf{p}=(p_1,p_2,\ldots,p_L)^T$ via Eqs. (1) and (2). As a result, $\mathbf{p}=(p_1,p_2,\ldots,p_L)^T$ can be used to describe the spectral variability of a pixel vector and its statistics of any order (mean, variance, skewness, kurtosis, etc.). For instance, we can define its statistics of different orders, such as the mean $\mu(\mathbf{r})=\sum_{l=1}^{L}p_l s_l$, variance $\sigma^2(\mathbf{r})=\sum_{l=1}^{L}p_l[s_l-\mu(\mathbf{r})]^2$, third central moment $\kappa^3(\mathbf{r})=\sum_{l=1}^{L}p_l[s_l-\mu(\mathbf{r})]^3$, fourth central moment $\kappa^4(\mathbf{r})=\sum_{l=1}^{L}p_l[s_l-\mu(\mathbf{r})]^4$, etc.

From information theory[5] we can further use $\mathbf{p}=(p_1,p_2,\ldots,p_L)^T$ to define the self-information provided by a particular band, say band j, by

$$I_j(\mathbf{r})=-\log p_j, \tag{3}$$

which describes how much information is yielded by the band image B_j. The entropy of a hyperspectral image pixel vector $\mathbf{r}$, denoted by $H(\mathbf{r})$, is actually the mean of the self-information over all bands and can be calculated by

$$H(\mathbf{r})=\sum_{j=1}^{L}I_j(\mathbf{r})p_j=-\sum_{j=1}^{L}p_j\log p_j, \tag{4}$$

which measures the uncertainty resulting from the pixel vector $\mathbf{r}$.

3 Spectral Discrimination Measures

In this section, three spectral discrimination measures are presented and used to measure the similarity between any two pixel vectors. Assume pixel vectors $\mathbf{r}$ and $\mathbf{r}'$ with their respective spectral signatures given by $\mathbf{s}=(s_1,s_2,\ldots,s_L)^T$ and $\mathbf{s}'=(s_1',s_2',\ldots,s_L')^T$.

3.1 *Spectral Information Divergence*[1]

Let $\mathbf{p}=(p_1,p_2,\ldots,p_L)^T$ and $\mathbf{q}=(q_1,q_2,\ldots,q_L)^T$ be the two probability mass functions generated by $\mathbf{s}=(s_1,s_2,\ldots,s_L)^T$ and $\mathbf{s}'=(s_1',s_2',\ldots,s_L')^T$, the spectral signatures of $\mathbf{r}$ and $\mathbf{r}'$, respectively. So the self-information provided by $\mathbf{r}'$ for band j is defined by Eq. (3) and given by

$$I_j(\mathbf{r}')=-\log q_j. \tag{5}$$

Using Eqs. (3) and (5), the discrepancy in the self-information of the band image B_j in $\mathbf{r}$ relative to the self-information of B_j in $\mathbf{r}'$, denoted by $D_j(\mathbf{r}\|\mathbf{r}')$, can be defined as

$$D_j(\mathbf{r}\|\mathbf{r}')=I_j(\mathbf{r})-I_j(\mathbf{r}')=\log(p_j/q_j). \tag{6}$$

Averaging $D_j(\mathbf{r}\|\mathbf{r}')$ in Eq. (6) over all the band images $\{B_l\}_{l=1}^{L}$ with respect to $\mathbf{r}$ results in

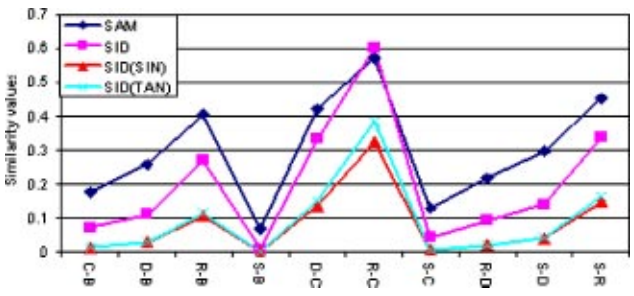

Fig. 2 Graphical plots of Tables 1 and 2.

Table 3 RSDPW values of SAM and SID using sagebrush as the reference signature.

		SAM			
		Blackbrush	Creosote leaves	Dry grass	Red soil
SID	Blackbrush	0	1.892 805	4.358 297	6.629 956
	Creosote leaves	4.809 524	0	2.302 56	3.502 715
	Dry grass	15.444 44	3.211 221	0	1.521226
	Red soil	37.142 86	7.722 772	2.404 933	0

Table 4 RSDPW values of SID(SIN) and SID(TAN) using red soil as the reference signature.

		SID(SIN)			
		Blackbrush	Creosote leaves	Dry grass	Red soil
SID(TAN)	Blackbrush	0	9.162 602	67.494 31	243.15 28
	Creosote leaves	9.172 358	0	7.366 282	26.537 53
	Dry grass	68.164 23	7.431 484	0	3.602 568
	Red soil	257.6992	28.0952	3.780 563	0

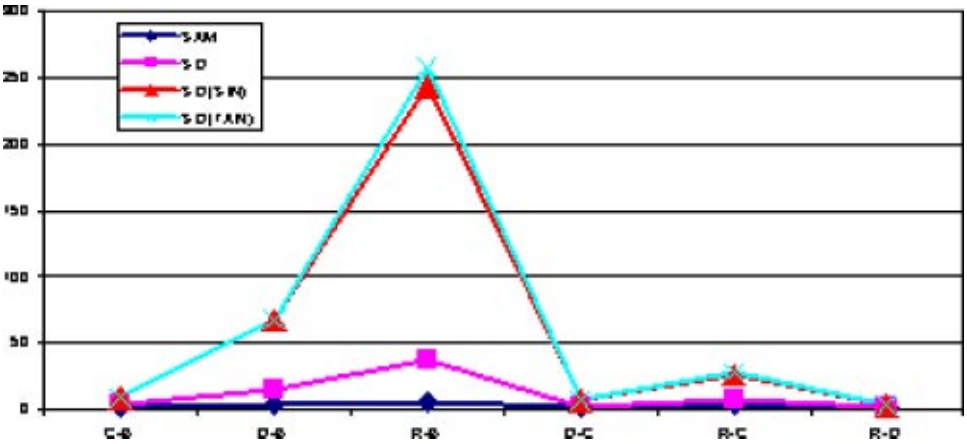

Fig. 3 Graphical plots of Tables 4 and 5.

Table 5 RSDPB and self-information values generated by SAM, SID, SID(SIN), and SID(TAN).

		Value					
Measure	Quantity	Blackbrush	Creosote leaves	Dry grass	Red soil	Sagebrush	Entropy
SAM	RSDPB	0.2266	0.3446	0.1074	0.0624	0.2589	
	Self-information	0.485 33	0.5297	0.3457	0.2497	0.5047	2.1151
SID	RSDPB	0.1879	0.4953	0.0549	0.0132	0.2486	
	Self-information	0.453 21	0.5021	0.2299	0.0824	0.4992	1.7668
SID(SIN)	RSDPB	0.1519	0.5953	0.0213	0.003	0.2284	
	Self-information	0.412 99	0.4455	0.1183	0.0251	0.4866	1.4885
SID(TAN)	RSDPB	0.1452	0.6106	0.0196	0.0027	0.2218	
	Self-information	0.4042	0.434 56	0.1112	0.0230	0.4819	1.4549

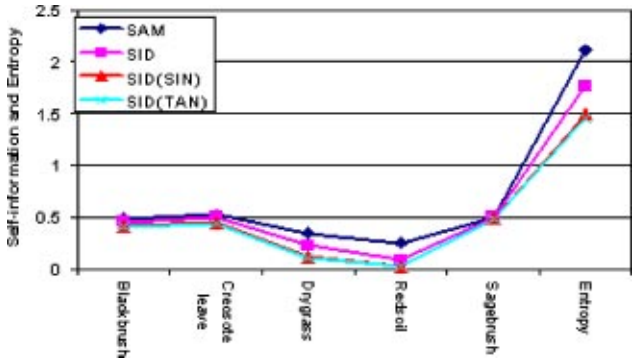

Fig. 4 Graphical plots of self-information values and entropies in Table 5.

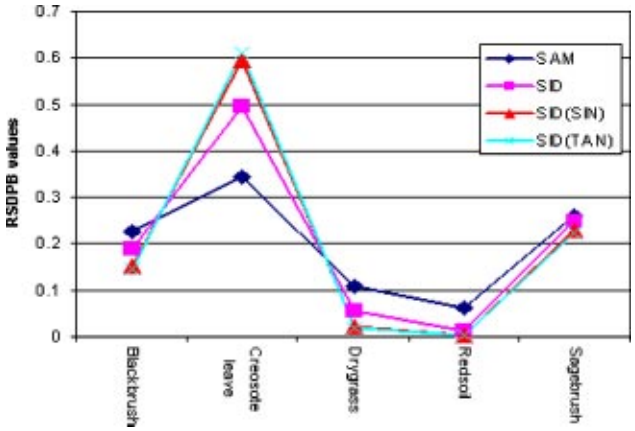

Fig. 5 Graphical plots of RSDPB values in Table 5.

$$D(\mathbf{r}\|\mathbf{r}')=\sum_{j=1}^{L} D_j(\mathbf{r}\|\mathbf{r}')p_j=\sum_{j=1}^{L} p_j\log(p_j/q_j), \tag{7}$$

where $D(\mathbf{r}\|\mathbf{r}')$ is the average discrepancy in the self-information of $\mathbf{r}'$ relative to that of $\mathbf{r}$. In context of information theory, $D(\mathbf{r}\|\mathbf{r}')$ in Eq. (7) is called the relative entropy of $\mathbf{r}'$ with respect to $\mathbf{r}$; it is also known as the Kullback-Leibler information measure, directed divergence, or cross entropy.[6] Similarly, we can also define the average discrepancy in the self-information of $\mathbf{r}$ relative to the self-information of $\mathbf{r}'$ by

$$D(\mathbf{r}'\|\mathbf{r})=\sum_{j=1}^{L} D_j(\mathbf{r}'\|\mathbf{r})q_j=\sum_{j=1}^{L} q_j\log(q_j/p_j). \tag{8}$$

Adding Eqs. (7) and (8) yields the *spectral information divergence* (SID), defined by

$$\mathrm{SID}(\mathbf{r},\mathbf{r}')=D(\mathbf{r}\|\mathbf{r}')+D(\mathbf{r}'\|\mathbf{r}), \tag{9}$$

which can be used to measure the discrepancy between two pixel vectors $\mathbf{r}$ and $\mathbf{r}'$ in terms of their corresponding probability mass functions $\mathbf{p}$ and $\mathbf{q}$. It should be noted that while $\mathrm{SID}(\mathbf{r},\mathbf{r}')$ is symmetric, $D(\mathbf{r}\|\mathbf{r}')$ is not. That is, $\mathrm{SID}(\mathbf{r},\mathbf{r}')=\mathrm{SID}(\mathbf{r}',\mathbf{r})$ and $D(\mathbf{r}\|\mathbf{r}')\neq D(\mathbf{r}'\|\mathbf{r})$.

3.2 *Spectral Angle Mapper*[7]

The SAM measures spectral similarity by finding the angle between the spectral signatures $\mathbf{s}$ and $\mathbf{s}'$ of two pixel vectors, $\mathbf{r}$ and $\mathbf{r}'$:

$$\mathrm{SAM}(\mathbf{s},\mathbf{s}')=\cos^{-1}\left(\frac{\langle\mathbf{s},\mathbf{s}'\rangle}{\|\mathbf{s}\|\,\|\mathbf{s}'\|}\right), \tag{10}$$

where $\langle\mathbf{s},\mathbf{s}'\rangle=\Sigma_{l=1}^{L}s_l s_l'$, $\|\mathbf{s}\|=(\Sigma_{l=1}^{L}s_l^2)^{1/2}$ and $\|\mathbf{s}'\|=[\Sigma_{l=1}^{L}(s_l')^2]^{1/2}$.

3.3 *SID-SAM Mixed Measure*

A new hyperspectral measure is introduced by combing the SID and SAM into a new measure, referred to as the SID-SAM mixed measure, which can be implemented in two versions. The first version is obtained by multiplying the SID by the tangent of the SAM between two spectral signatures $\mathbf{s}$ and $\mathbf{s}'$ and is given by

$$\mathrm{SID(TAN)}=\mathrm{SID}(\mathbf{s},\mathbf{s}')\times\tan(\mathrm{SAM}(\mathbf{s},\mathbf{s}')). \tag{11}$$

The second version replaces the tangent function in Eq. (11) with the sine function and yields the following new measure:

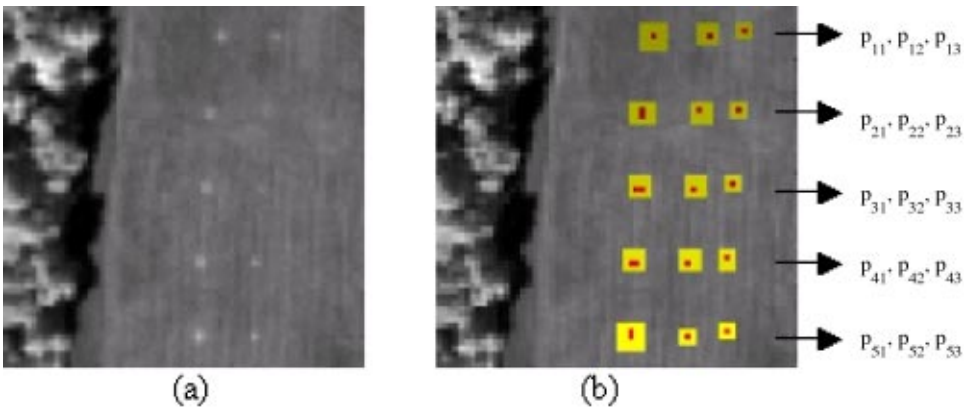

Fig. 6 (a) A HYDICE panel scene that contains 15 panels; (b) ground truth map of the spatial locations of the 15 panels

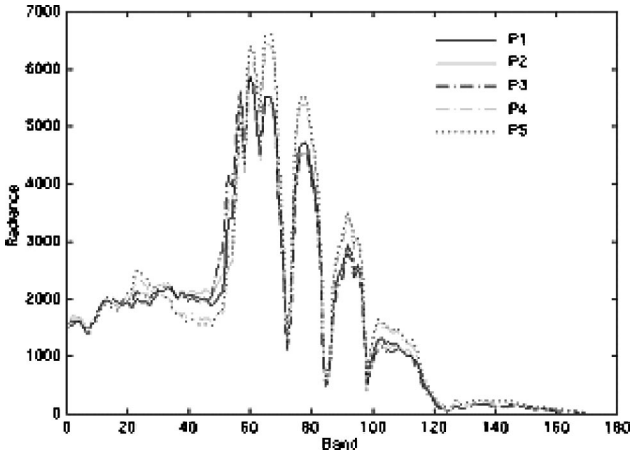

Fig. 7 Spectra of P1, P2, P3, P4, and P5.

$$\mathrm{SID(SIN)} = \mathrm{SID}(\mathbf{s},\mathbf{s}') \times \sin(\mathrm{SAM}(\mathbf{s},\mathbf{s}')), \tag{12}$$

which is the product of the SID and the sine of the SAM between two spectral signatures $\mathbf{s}$ and $\mathbf{s}'$.

By taking the product of two measures, the SAM and the SID, the spectral discriminability of the new SID-SAM mixed measure is increased considerably because it makes two similar spectral signatures even more similar and two dissimilar spectral signatures more distinct. However, if the cosine function is used to replace the sine function in Eq. (12), the spectral discriminability will be significantly reduced, because the cosine calculates the projection of one spectral signature along the other one instead of the projection of one spectral signature orthogonal to the other.

4 Measures of Spectral Discriminability

In this section, we briefly review three measures proposed in Refs. 1 and 2 that can be used to evaluate the effectiveness of a discrimination measure in terms of the spectral discriminatory probability and power.

4.1 *Relative Spectral Discriminatory Probability (RSDPB)*

Let $\{\mathbf{s}_k\}_{k=1}^K$ be K spectral signatures specified by a given set Δ, which can be considered as either a database or a spectral library. Also assume that $\mathbf{t}$ is any specific target spectral signature to be identified via Δ. We define the spectral discriminatory probabilities of all s_k's in Δ with respect to $\mathbf{t}$ by

Table 6 Discrimination values produced by SAM and SID.

		SAM				
		P1	P2	P3	P4	P5
SID	P1	—	0.0435	0.0673	0.1144	0.1240
	P2	0.0039	—	0.0430	0.1479	0.1567
	P3	0.0086	0.0033	—	0.1652	0.1710
	P4	0.0233	0.0385	0.0476	—	0.0248
	P5	0.0313	0.0485	0.0570	0.0025	—

Table 7 Discrimination values produced by SID(SIN) and SID(TAN).

		SID(SIN)				
		P1	P2	P3	P4	P5
SID(TAN)	P1	—	0.0002	0.0006	0.0027	0.0039
	P2	0.0002	—	0.0001	0.0057	0.0076
	P3	0.0006	0.0001	—	0.0078	0.0097
	P4	0.0027	0.0057	0.0079	—	0.0001
	P5	0.0039	0.0077	0.0098	0.0001	—

$$p_{\mathbf{t},\Delta}^m(k) = \frac{m(\mathbf{t},\mathbf{s}_k)}{\sum_{i=1}^K m(\mathbf{t},\mathbf{s}_i)} \quad \text{for } k = 1,2,...,K, \tag{13}$$

where $\sum_{i=1}^K m(\mathbf{t},\mathbf{s}_i)$ is a normalization constant determined by $\mathbf{t}$ and Δ. The resulting probability vector $\mathbf{p}_{\mathbf{t},\Delta}^m = (p_{\mathbf{t},\Delta}^m(1), p_{\mathbf{t},\Delta}^m(2),\ldots,p_{\mathbf{t},\Delta}^m(K))^T$ is called *relative spectral discriminatory probability* (RSDPB) of Δ with respect to $\mathbf{t}$, or the spectral discriminatory probability vector of Δ relative to $\mathbf{t}$.

Using Eq. (13) we can identify $\mathbf{t}$ by selecting the member of Δ with the smallest relative spectral discriminability probability. If there is a tie, any tied member can be used for $\mathbf{t}$.

4.2 *Relative Spectral Discriminatory Entropy (RSDE)*

Since $\mathbf{p}_{\mathbf{t},\Delta}^m = (p_{\mathbf{t},\Delta}^m(1), p_{\mathbf{t},\Delta}^m(2),\ldots,p_{\mathbf{t},\Delta}^m(K))^T$ given by Eq. (13) is the relative spectral discriminatory probability vector of $\mathbf{t}$ using a selective set of spectral signatures, $\Delta = \{\mathbf{s}_k\}_{k=1}^K$, we can further define the *relative spectral discriminatory entropy* (RSDE) of the spectral signature $\mathbf{t}$ with respect to the set Δ, denoted by $H_{\mathrm{RSDE}}^m(\mathbf{t},\Delta)$, as follows:

$$H_{\mathrm{RSDE}}^m(\mathbf{t},\Delta) = -\sum_{k=1}^K p_{\mathbf{t},\Delta}^m(k) \log_2 p_{\mathbf{t},\Delta}^m(k). \tag{14}$$

Equation (14) provides a measure of the uncertainty of identifying $\mathbf{t}$ by using $\Delta = \{\mathbf{s}_k\}_{k=1}^K$. A larger $H_{\mathrm{RSDE}}^m(\mathbf{t},\Delta)$ may have a smaller chance of identifying $\mathbf{t}$.

4.3 *Relative Spectral Discriminatory Power (RSDPW)*

Assume that $m(\ ,\ )$ is any given hyperspectral measure such as the SID, SAM, or SID-SAM mixed measure. Let $\mathbf{d}$

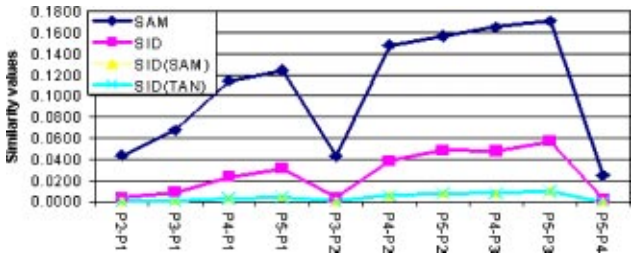

Fig. 8 Graphical plots of Tables 6 and 7.

Table 8 RSDPB and self-information values generated by SAM, SID, SID(SIN), and SID(TAN) using p_{23}.

Measure	Quantity	Value					
		P1	P2	P3	P4	P5	Entropy
SAM	RSDPB	0.1309	0.0670	0.1284	0.3259	0.3477	
	Self-information	0.3840	0.2613	0.3802	0.5271	0.5299	2.0826
SID	RSDPB	0.0705	0.0200	0.0536	0.3786	0.4773	
	Self-information	0.2697	0.1129	0.2263	0.5305	0.5093	1.6487
SID(SIN)	RSDPB	0.0302	0.0044	0.0225	0.4022	0.5407	
	Self-information	0.1525	0.0344	0.1232	0.5285	0.4797	1.3182
SID(TAN)	RSDPB	0.0298	0.0043	0.0223	0.4020	0.5415	
	Self-information	0.1510	0.0338	0.1224	0.5285	0.4792	1.3149

be the spectral signature of a reference pixel vector. Suppose that $\mathbf{s}$ and $\mathbf{s}'$ are the spectral signatures of any pair of pixel vectors. The RSDPW of $m(\,,\,)$, denoted by $\mathrm{RSDPW}^m(\mathbf{s},\mathbf{s}';\mathbf{d})$, is then defined by

$$\mathrm{RSDPW}^m(\mathbf{s},\mathbf{s}';\mathbf{d}) = \max\left\{\frac{m(\mathbf{s},\mathbf{d})}{m(\mathbf{s}',\mathbf{d})}, \frac{m(\mathbf{s}',\mathbf{d})}{m(\mathbf{s},\mathbf{d})}\right\}. \tag{15}$$

More precisely, $\mathrm{RSDPW}^m(\mathbf{s},\mathbf{s}';\mathbf{d})$ calculates two ratios—the ratio of $m(\mathbf{s},\mathbf{s}';\mathbf{d})$ to $m(\mathbf{s}',\mathbf{s};\mathbf{d})$ and the ratio of $m(\mathbf{s}',\mathbf{s};\mathbf{d})$ to $m(\mathbf{s},\mathbf{s}';\mathbf{d})$—and selects the greater of them as the discriminatory power of $m(\,,\,)$. The function $\mathrm{RSDPW}^m(\mathbf{s},\mathbf{s}';\mathbf{d})$ defined by Eq. (15) provides a quantitative index of the spectral discrimination ability of a specific hyperspectral measure $m(\,,\,)$ between two spectral signatures $\mathbf{s}$ and $\mathbf{s}'$ relative to $\mathbf{d}$. Obviously, the higher $\mathrm{RSDPW}^m(\mathbf{s},\mathbf{s}';\mathbf{d})$ is, the better the discriminatory power of $m(\,,\,)$ is. In addition, $\mathrm{RSDPW}^m(\mathbf{s},\mathbf{s}';\mathbf{d})$ is symmetric and bounded below by 1, i.e., $\mathrm{RSDPW}^m(\mathbf{s},\mathbf{s}';\mathbf{d}) \geqslant 1$, with equality if and only if $\mathbf{s}=\mathbf{s}'$.

5 Experiments

Two data sets were used for experiments. The first was the AVIRIS (Airborne Visible/Infrared Imaging Spectrometer) reflectance data shown in Fig. 1(a), consisting of five field reflectance spectra (blackbrush, creosote leaves, dry grass, red soil, and sagebrush) with a spectral coverage from 0.4 to 2.5 μm. Only 158 bands were left after the water bands were removed. Using these five signatures, we calculated the discrimination values for four spectral measures: the SAM, the SID, the SID(TAN), and the SID(SIN). Table 1 tabulates the results for the SAM and the SID, where the values in the upper triangular matrix were generated by the SAM and the values in the lower triangular matrix were produced by the SID. Similarly, the values generated by the SID(SIN) and the SID(TAN) are tabulated in the upper and lower triangular matrices of Table 2, respectively. It is difficult to see which measure is more effective, merely from a comparison between Table 1 and Table 2. Thus, Fig. 2 also plots the values in Tables 1 and 2 for visual comparison. However, despite the fact that the SID(TAN) and the SID(SIN) yielded smaller values than those produced by the SAM and the SID, we cannot conclude that a larger spectral similarity value means better discriminatory power.

In order to remedy this diffuculty, we calculate the relative spectral discriminatory power defined by Eq. (15) using sagebrush as the reference signature $\mathbf{d}$ as shown in Fig. 1(b). We selected sagebrush for this purpose because sagebrush is very close to both blackbrush and creosote leaves, as shown in Tables 1 and 2, and provides a good case to evaluate the effectiveness of a spectral measure. Tables 3 and 4 tabulate their results. As we can see from these two tables, the proposed SID(TAN) and SID(SIN) performed significantly better than the SID and the SAM. Figure 3 plots their RSDPW values, which also clearly indicate the superior performance of the SID(TAN) and the SID(SIN) to the SID and the SAM. For example, the spectral signatures of sagebrush, blackbrush, and creosote leaves are very

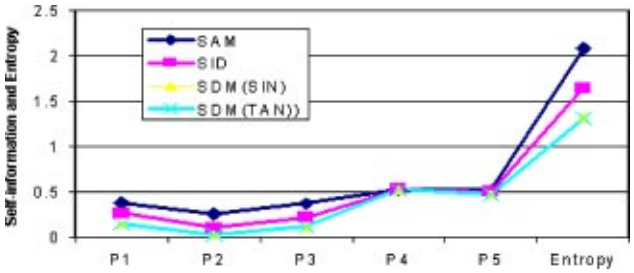

Fig. 9 Graphical plots of RSDPB values in Table 8.

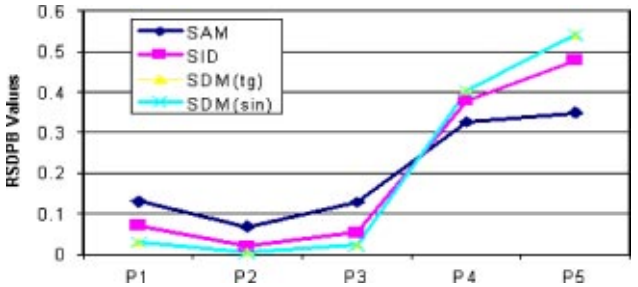

Fig. 10 Graphical plots of self-information values and entropies in Table 8.

Table 9 RSDPW values of SAM and SID using P2 as the reference signature.

		SAM			
		P1	P3	P4	P5
SID	P1	—	1.0116	3.4000	3.6023
	P3	1.1818	—	3.4395	3.6442
	P4	9.8718	11.6667	—	1.0595
	P5	12.4103	14.6667	1.2571	—

Table 10 RSDPW values of SID(SIN) and SID(TAN) using P2 as the reference signature.

		SID(SIN)			
		P1	P3	P4	P5
SID(TAN)	P1	—	2.0000	28.5000	38.0000
	P3	2.0000	—	57.0000	76.0000
	P4	28.5000	57.0000	—	1.3333
	P5	38.5000	77.0000	1.3509	—

close according to Fig. 1. As expected, the spectral discrimination among these three is difficult. Apparently, based on our experiments, the SAM was the worst, with discriminatory power 1.892 805. The SID improved on the discriminatory power of the SAM by 2.5 times; for the SID-SAM mixed measure the discriminatory power was almost 5 times that of the SAM and twice that of the SID. It is worth noting that the RSDPW values between dry grass and red soil are very small among all the four measures. This is mainly because the sagebrush, which was selected as the reference signature, has a very distinct spectral signature from those of dry grass and red soil. As a result, the RSDPW values yielded by the four measures were relatively small, which implies that the discriminatory power between dry grass and sagebrush was nearly the same as that between red soil and sagebrush. These results also suggested that the dry grass and red soil have very distinct signatures from the signature of sagebrush.

In order to further evaluate the ability of the mixed measures in discriminatory power against a reference signature, we used the same target signature used in Ref. 1, which is a mixed signature composed of 0.1055 blackbrush, 0.0292 creosote leaves, 0.0272 dry grass, 0.7588 red soil, and 0.0974 sagebrush. Table 5 tabulates the RSDPB and self-information values with their entropies for the signatures; the proposed SID-SAM mixed measures, SID(SIN) and SID(TAN), yielded the two smallest entropies. Plots of comparisons among these four measures are also shown in Figs. 4 and 5, where the proposed SID(SIN) and SID(TAN) clearly have better spectral discriminability in identifying the target signature **t** as red soil, with smaller spectral discriminatory probabilities than those produced by the SID and the SAM.

The data in the second set to be used in the experiments are real HYDICE (Hyperspectral Digital Image Collection Experiment) data. A HYDICE image scene is shown in Fig. 6(a) (band 80) with the ground truth map in Fig. 6(b). The spatial positions of these 15 panels are precisely located, with black (B) pixels indicating the panel center pixels of all the 15 panels, and white (W) pixels being panel pixels mixed with background pixels. In this case, a W pixel can be considered as a mixed pixel. The scene has size 64 $\times$64 pixels; the low-signal, high-noise bands (bands 1 to 3 and bands 202 to 210), and water vapor absorption bands (bands 101 to 112 and bands 137 to 153) have been removed. The 15 panels are arranged in a 5×3 matrix. Each element in this matrix is a square panel and denoted by p_{ij} with row indexed by $i=1,\ldots,5$ and column indexed by $j=1,2,3$. For each row $i=1,\ldots,5$, the three panels p_{i1},p_{i2},p_{i3} were painted with the same material but have three different sizes. For each column $j=1,2,3$, the five panels $p_{1j},p_{2j},p_{3j},p_{4j},p_{5j}$ have the same size but were painted by five different materials. The sizes of the panels in the first, second, and third columns are 3m$\times$3m, 2m $\times$2m, and 1m$\times$1m, respectively. The 15 panels have five different materials and three different sizes. Figure 7 plots the five panel spectral signatures $\{\mathrm{P}i\}_{i=1}^{5}$ obtained from Fig. 6(b), where the i'th panel signature, denoted by Pi, was generated by averaging all B pixels in row I and was used to represent target knowledge of the panels in row i. The 1.5-m spatial resolution of the image scene suggests that except for $p_{21},p_{31},p_{41},p_{51}$, which are two-pixel panels, all the rest of the 11 panels are single-pixel panels.

As with the AVIRIS data studied previously, we conducted similar experiments using these five panel signatures. Tables 6 and 7 tabulate spectral discrimination values of the SAM, the SID, the SID(SIN), and the SID(TAN); the values in the upper triangular matrices were generated by the SAM and the SID(SIN), respectively, while the values in the lower triangular matrices were produced by the SID and the SID(TAN), respectively. As expected, the values of the proposed SID(SIN) and SID(TAN) were also smaller than those produced by the SAM and the SID. In analogy with Fig. 2, Fig. 8 plots the values in Tables 6 and 7 for graphical comparison. Once again, we also calculated the RSDPB and self-information values among the five panel signatures and their entropies. The results are tabulated in Table 8, with their corresponding graphical plots in Figs. 9 and 10. As shown in these tables and Fig. 9, the proposed SID(SIN) and SID(TAN) again produced the smallest entropies. The RSDPW values of the four measures are tabulated in Tables 9 and 10, and their corresponding graphical plots are in Fig. 11, where the reference signature **d** was chosen to be the panel signature p_{23}. As shown, the RSDPW values of the proposed SID(SIN) and SID(TAN) yielded better discriminatory powers than did the SID and

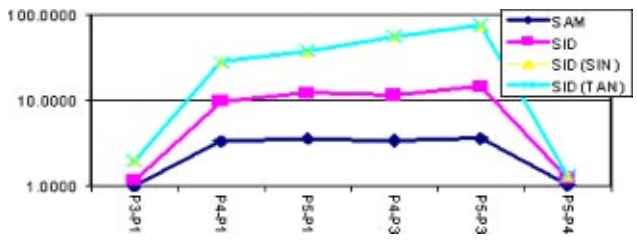

Fig. 11 Graphical plots of RSDPW values in Tables 9 and 10.

the SAM. The magnitude of the improved power is proportional to the dissimilarity between the signatures and the reference signature.

6 Conclusions

This paper presents a new hyperspectral discrimination measure, the SID-SAM mixed measure, which is a mixture of the widely used spectral angle mapper (SAM) and a recently developed information measure, the spectral information divergence (SID). Despite the fact that the SID-SAM mixed measure is obtained by simply multiplying the SID by the SAM, the improvement on the performance in spectral discriminability is remarkable, as demonstrated in experiments. As a result, two similar spectral signatures are made more similar, while two dissimilar spectral signatures become more distinct. This is because the measure combines the strengths of SAM and SID.

Acknowledgment

The second and third authors acknowledge support received from their NRC (National Research Council) senior and postdoctoral research associateships sponsored by the U.S. Army Soldier and Biological Command, Edgewood Chemical and Biological Center (ECBC).

References

1. C.-I. Chang, ''An information theoretic-based approach to spectral variability, similarity and discriminability for hyperspectral image analysis,'' *IEEE Trans. Inf. Theory* **46**(5), 1927–1932 (2000).
2. C.-I. Chang, *Hyperspectral Imaging: Techniques for Spectral Detection and Classification*, Chapter 2, Kluwer Academic/Plenum Publishers, New York (2003).
3. C.-I. Chang and C. Brumbley, ''Linear unmixing Kalman filtering approach to signature abundance detection, signature estimation and subpixel classification for remotely sensed images,'' *IEEE Trans. Aerosp. Electron. Syst.* **37**(1), 319–330 (1999).
4. Q. Du and C.-I. Chang, ''A hidden Markov model approach to spectral analysis for hyperspectral imagery,'' *Opt. Eng.* **40**(10), 2277–2284 (2001).
5. T. Cover and J. Thomas, *Elements of Information Theory*, Wiley, New York (1991).
6. S. Kullback, *Information Theory and Statistics*, Dover, Gloucester, MA (1968).
7. R. A. Schowengerdt, *Remote Sensing: Models and Methods for Image Processing*, 2nd ed., Academic Press, San Diego (1997).

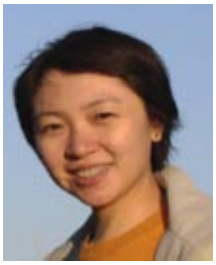

Yingzi Du is an assistant research professor in the Electrical Engineering Department at the United States Naval Academy. She earned her PhD in electrical engineering from the University of Maryland, Baltimore County, in 2003. She received her BS and MS degrees in electrical engineering from Beijing University of Posts and Telecommunications in 1996 and 1999, respectively. Her research interests include biometrics, multispectral/hyperspectral image processing, video image processing, medical imaging, and pattern recognition. Dr. Du is a member of SPIE and IEEE, a life member of Phi Kappa Phi, and a member of Tau Beta Pi.

Chein-I Chang received his BS degree from Soochow University, Taipei, Taiwan, MS degree from the Institute of Mathematics at National Tsing Hua University, Hsinchu, Taiwan, and MA degree from the State University of New York at Stony Brook, all in mathematics. He received his MS and MSEE degrees from the University of Illinois at Urbana-Champaign, and PhD degree in electrical engineering from the University of Maryland, College Park. Dr. Chang has been with the University of Maryland, Baltimore County (UMBC) since 1987, as a visiting assistant professor from January to August 1987, assistant professor from 1987 to 1993, associate professor from 1993 to 2001, and professor in the Department of Computer Science and Electrical Engineering since 2001. He was a visiting research specialist in the Institute of Information Engineering at the National Cheng Kung University, Tainan, Taiwan, from 1994–1995. He received an NRC (National Research Council) senior research associateship award from 2002 to 2003 sponsored by the U.S. Army Soldier and Biological Chemical Command, Edgewood Chemical and Biological Center, Aberdeen Proving Ground, Maryland. He has three patents and several pending patents on image-processing techniques for hyperspectral imaging and detection of microcalcifications. He is on the editorial board and was the guest editor of a special issue on telemedicine and applications of the *Journal of High Speed Networks*. His research interests include automatic target recognition, multispectral/hyperspectral image processing, medical imaging, and visual information systems. He is the author of a book, *Hyperspectral Imaging: Techniques for Spectral Detection and Classification*, published by Kluwer Academic/Plenum Publishers. Dr. Chang is an associate editor in the area of hyperspectral signal processing for *IEEE Transactions on Geoscience and Remote Sensing*. He is a senior member of the IEEE and a member of Phi Kappa Phi and Eta Kappa Nu.

Hsuan Ren received the BS degree in electrical engineering from the National Taiwan University, Taipei, Taiwan, R.O.C., in 1994, and the MS and PhD degrees from University of Maryland, Baltimore County in 1998 and 2000, respectively, all in electrical engineering. He received a National Research Council (NRC) postdoctoral research associateship award supported by U.S. Army Edgewood Chemical Biological Center from 2000 to 2003. He is currently an assistant professor of Information Engineering and with the Center for Space and Remote Sensing Research in National Central University, Chung-Li, Taiwan, R.O.C. He received the third paper prize award in the student paper prize competition at the IEEE International Geoscience and Remote Sensing Symposium 2000, and also was one of four finalists in the student paper prize competition at the IEEE International Geoscience and Remote Sensing Symposium 1998. Dr. Ren has two patents pending on hyperspectral target detection and image classification. His research interests include data compression, signal and image processing, and pattern recognition. He is a member of the IEEE and SPIE. He is also a member of the honor society Phi Kappa Phi.

Chein-Chi Chang received the BS degree from Tamkang University, Taiwan, 1979; the MS degree from the Ohio State University, 1981; and the PhD degree in civil engineering from the University of Missouri–Rolla, 1988. Dr. Chang has been a senior engineer with District of Columbia Water and Sewer Authority (WASA) since 2000. Prior to joining the WASA, Dr. Chang was a licensed professional engineer in the State of Maryland and the District of Columbia and worked for several engineering consulting companies. He has been an adjunct professor affiliated with four universities: University of Maryland Baltimore County, University of Northern Virginia, China Hunan University, and China Central South University. He has been

very active in several engineering societies: the American Society of Civil Engineers, the Chinese Institute of Engineers—USA, and the Overseas Chinese Environmental Engineers and Scientists Association. His research interests include multispectral/hyperspectral image processing in environmental applications, system optimization, remote sensing, geographic information systems, and water resources engineering.

Biographies and photographs of the other authors not available.